Structural Studies on the Membrane-Bound Immunoglobulin E–Receptor Complex. 2. Mapping of Distances between Sites on IgE and the Membrane Surface†

David Holowka and Barbara Baird*

ABSTRACT: Resonance energy transfer has been used to investigate the structure of IgE bound to receptors on the plasma membrane of rat basophilic leukemia (RBL) cells. Isolated monoclonal IgE has been labeled with donor probes in two different regions: fluorescein 5-isothiocyanate preferentially labels the Fab segments, and limited reduction followed by alkylation with *N*-[4-[7-(diethylamino)-4-methylcoumarin-3-yl]phenyl]maleimide causes selective modification of the inter ϵ chain disulfides in the $C_\epsilon2$ domains. These donor-labeled IgE molecules bind with characteristic high affinity to large, oriented plasma membrane vesicles prepared from RBL cells, and amphipathic acceptor probes can be titrated into these vesicles at surface densities that can be directly measured. Two different acceptor probes for each donor have been used. From fluorescence quenching of the donor probes measured as a function of acceptor density, the effective distance from the membrane surface has been determined to be 71–106 Å for the fluorescein-labeled Fab segments and 35–52 Å for the coumarin-labeled $C_\epsilon2$ domains. This information is used together with that from recent biochemical studies to propose new models for the structural orientation of membrane receptor-bound IgE.

Immunoglobulin E (IgE)[1] bound to its receptor on the surface of mast cells and basophils mediates the triggering of cellular degranulation by multivalent antigen, and this process initiates the allergic response (Ishizaka & Ishizaka, 1975; Siraganian, 1981). The receptor for IgE on these cells is an intrinsic membrane protein containing at least two subunits, a glycopeptide of $M_r \approx 50\,000$ (α) which has the binding site for IgE (Conrad & Froese, 1976; Kulczycki et al., 1976) and a polypeptide of $M_r \approx 35\,000$ (β) which interacts strongly with the membrane bilayer (Holowka et al., 1980; Holowka & Metzger, 1982). Some information concerning the interaction between bound IgE and its receptor has been accumulated. The association is monovalent (Kanellopoulos et al., 1980) and very tight ($K_a \geq 10^{10}$ M^{-1}; Kulczycki & Metzger, 1974; Sterk & Ishizaka, 1982) and apparently does not involve the carbohydrate residues on α (Pecoud et al., 1981) which comprise about 30% of the mass of that subunit (Kanellopoulos et al., 1980) nor does it depend on the presence of the β subunit (Kanellopoulos et al., 1980; Holowka & Metzger, 1982). Studies on human IgE have demonstrated that the F_c fragment composed of the disulfide-linked dimer ($C_\epsilon2$ $C_\epsilon3$ $C_\epsilon4$)$_2$ contains the region of interaction between IgE and the receptor, while the F(ab′)$_2$ fragment (which contains the $C_\epsilon2$ domains as well as the two Fab segments) does not bind significantly (Ishizaka et al., 1970; Dorrington & Bennich, 1978). Circular dichroism studies of thermal denaturation of human IgE have shown that the $C_\epsilon3$ domain contains the major contribution to the irreversible unfolding at 56 °C which correlates with the loss of receptor binding activity under these conditions (Dorrington & Bennich, 1978). Recent studies on rodent IgE have revealed that a site of trypsin cleavage between $C_\epsilon2$ and $C_\epsilon3$ domains of rat IgE is markedly protected from proteolysis when that IgE is receptor bound but a site in the middle of the $C_\epsilon3$ domain is only marginally affected (Perez-Montfort & Metzger, 1982). All of these results are consistent with the hypothesis that a limited region of the $C_\epsilon3$ domain, apparently near the $C_\epsilon2$–$C_\epsilon3$ interface, is involved in the binding of IgE to its receptor on mast cells, basophils, or the tumor analogue, rat basophilic leukemia (RBL) cells.

In order to obtain a more detailed molecular picture of the structure of the membrane-bound IgE–receptor complex we have begun to employ quantitative fluorescence methods. In particular we are using resonance energy-transfer measurements to map distances between sites on the bound IgE molecule and the membrane surface. Our experimental system employs monoclonal mouse IgE that we have selectively modified with donor probes in two different regions, the $C_\epsilon2$ domains and the Fab segments. These labeled IgE molecules bind tightly to receptors in large, oriented plasma membrane vesicles prepared from RBL cells as described in the preceding paper (Holowka & Baird, 1983), and amphipathic acceptor probes can be inserted into the membrane bilayer at measureable densities. The distances determined from our energy-transfer studies have provided some new information by imposing restrictions on the possible structural arrangements of the receptor-bound IgE.

Experimental Procedures

Chemicals. The fluorescent probes HAF, HAE, ORB, FITC, and $DiOC_{10}$-(3) were obtained as described in the preceding paper (Holowka & Baird, 1983). *N*-[4-[7-(Diethylamino)-4-methylcoumarin-3-yl]phenyl]maleimide (CPM) and 5-[[2-[(iodoacetyl)amino]ethyl]amino]naphthalene-1-sulfonic acid (IAEDANS) were obtained from Molecular

† From the Department of Chemistry, Baker Laboratory, Cornell University, Ithaca, New York 14853. *Received December 28, 1982.* This work was supported by research grants from the American Chemical Society (PRF 12717), Research Corporation (Cottrell Grant), and the National Institutes of Health (AI 18306).

[1] Abbreviations: IgE, immunoglobulin E; RBL, rat basophilic leukemia; HAF, 5-(hexadecanoylamino)fluorescein; ORB, octadecylrhodamine B chloride; FITC, fluorescein 5-isothiocyanate; CPM, *N*-[4-[7-(diethylamino)-4-methylcoumarin-3-yl]phenyl]maleimide; IAEDANS, 5-[[2-[(iodoacetyl)amino]ethyl]-5-amino]naphthalene-1-sulfonic acid; $DiOC_{10}$-(3), didecyloxacarbocyanine; DPCC, diphenylcarbamoyl chloride; Me_2SO, dimethyl sulfoxide; BBS, borate-buffered saline; PBS/NaN_3, phosphate-buffered saline with sodium azide; $NaDodSO_4$, sodium dodecyl sulfate; FITC–IgE, IgE that has been reacted with FITC; CPM–IgE(+), IgE that has been first reduced with dithiothreitol and then alkylated with CPM; CPM–IgE(−), IgE that has been reacted with CPM without prior reduction; Tris, tris(hydroxymethyl)aminomethane; EDTA, ethylenediaminetetraacetic acid; DNP, dinitrophenyl.

0006-2960/83/0422-3475$01.50/0 © 1983 American Chemical Society

Probes, Inc. [^{3}H]-*N*-Ethylmaleimide was obtained from New England Nuclear. Diphenylcarbamoyl chloride treated trypsin (DPCC-trypsin), chicken egg white ovomucoid, and papain (type III) were obtained from Sigma Chemical Co. Molecular weight standards for polyacrylamide gel electrophoresis were from Bio-Rad Laboratories.

Preparation of IgE Derivatives. Murine monoclonal anti-2,4-dinitrophenyl-IgE from the tumor HI DNP-ε-26-82 (Liu et al., 1980) was purified and labeled with ^{125}I as previously described (Holowka & Baird, 1983). FITC–IgE was prepared by reacting IgE (1×10^{-6} M) in borate-buffered saline (BBS; 0.2 M $NaBO_3$ and 0.16 M NaCl) at pH 9.1 with FITC [$(0.75–1.30) \times 10^{-4}$ M] for 16–24 h at 4 °C. FITC was either added directly to the IgE solution as a methanolic solution (final concentration of methanol was 0.5%) or added as a dimethyl sulfoxide (Me_2SO) solution to BBS which bathed a dialysis bag containing the IgE sample (final Me_2SO concentration was 0.2%). After reaction, samples were dialyzed extensively against several changes of BBS, pH 8.0. The concentration of bound FITC was determined from the OD at 495 nm by using an extinction coefficient (ε) which corresponded to the appropriate ratio of OD(495)/OD(470) from the data of Mercola et al. (1972). Values for ε ranged from 6.4×10^4 to 8.5×10^4 M^{-1} cm^{-1} for different preparations. The concentration of IgE for these derivatives was determined by the method of Lowry et al. (1951) by using a correction factor of 0.80 which is necessary to obtain the same concentration for unmodified IgE by using $\epsilon_{280nm}^{0.1\%} = 1.62$ (Liu et al., 1980). The molecular weight of IgE was assumed to be 184000 (Liu et al., 1980).

For selectively reduced and alkylated derivatives, IgE was incubated with 1 mM dithiothreitol for 1 h at ambient temperature in nitrogen-flushed 20 mM sodium phosphate and 0.1 M NaCl, pH 8.0. At the end of the reduction period, the pH was lowered to 7.5 by the addition of a small aliquot of 0.2 M NaH_2PO_4, and either [^{3}H]-*N*-ethylmaleimide in phosphate buffered saline or CPM in Me_2SO was added to final concentrations of 2.5 and 3.0 mM, respectively (the final concentration of Me_2SO was 5%). Alkylation reactions were carried out at ambient temperature for 1 h; the sample containing CPM was rocked gently in a Labquake shaker (Labindustries, Inc.). IgE that had not been reduced with dithiothreitol also was reacted with 1 mM CPM under these same conditions. At the end of the reaction period, the [^{3}H]-*N*-ethylmaleimide reaction mix (0.5 mL) was layered onto a 3-mL centrifuge column (Penefsky, 1977) of Sephadex G-25 Fine equilibrated with BBS, pH 8.0, and the labeled IgE was collected as the effluent after centrifugation at 200*g* for 2 min in a Sorvall GLC-2B centrifuge. The CPM-reacted samples were spun in a Beckman microfuge B (9000*g*) for 2 min to remove most of the insoluble CPM and CPM–dithiothreitol adduct. Samples were further clarified by filtration through a Millipore HAWP 01300 filter (0.45-μm pore size) by using a syringe with positive pressure and then passed through a centrifuge column as above to remove soluble non-IgE-bound CPM. Recovery of modified IgE was about 50% for both CPM–IgE derivatives: that which had undergone prior reduction with dithiothreitol [designated CPM–IgE(+)] and that which had not been reduced [designated CPM–IgE(−)]. The concentration of IgE-bound CPM was determined from the OD at 395 nm assuming $\epsilon = 3.0 \times 10^4$ M^{-1} cm^{-1} (Sippel, 1981). Correction was made for the small amount of CPM present which was not covalently bound (see footnote to Table I). The IgE concentration was determined from the OD at 280 nm, assuming no significant contribution from CPM at that wavelength (see Figure 2B).

Enzymatic Digestion and $NaDodSO_4$–Polyacrylamide Gel Electrophoresis Analysis of IgE Derivatives. Digestion of IgE derivatives (0.3 mg/mL) with DPCC–trypsin (2% w/w) was carried out in 40 mM Tris-HCl (pH 8.1) and 10 mM $CaCl_2$ at 37 °C. Aliquots from the digestion mixture were quenched with ovomucoid trypsin inhibitor (20-fold w/w excess over DPCC–trypsin) and cooled to 4 °C. Digestion with papain (2% w/w) was carried out by the procedure of Porter (1959) in 0.1 M sodium phosphate (pH 7.0), 10 mM cysteine hydrochloride, and 2 mM EDTA at 30 °C. The digestion was stopped by the addition of 15 mM *N*-ethylmaleimide and cooling to 4 °C. Samples were prepared for sodium dodecyl sulfate–polyacrylamide gel electrophoresis by mixing with an equal volume of 2% $NaDodSO_4$ (w/v), 20% glycerol (v/v), and 80 mM Tris-HCl, pH 6.8, and boiling for 2 min. Slab gels prepared by the method of Laemmli (1970) were employed for $NaDodSO_4$–polyacrylamide gel electrophoresis as previously described (Holowka et al., 1980) to analyze IgE derivatives before and after enzymatic digestion. Samples to be analyzed under reducing conditions were mixed with β-mercaptoethanol (2% v/v) and boiled for 1 min immediately prior to electrophoresis. Slabs containing fluorescent derivatives of IgE were examined and photographed immediately after electrophoresis with illumination from a near-ultraviolet light box which was filtered by a Corning glass plate CS 7-60 and a Kodak Wratten filter no. 2E. Polaroid 57 film was used for photography. Quantitative analysis of the fluorescence from individual bands was performed as follows: The bands were excised with a razor blade from nonfixed, nonstained gels under UV illumination, then ground to small pieces in 1% $NaDodSO_4$ and PBS, and incubated overnight at 37 °C with vigorous shaking. After the gel particles settled to the bottom of the test tube, an aliquot of the supernatant was withdrawn for fluorescence measurement (see below). Greater than 90% of the fluorescence was recovered from the gel by this procedure. [^{3}H]-*N*-Ethylmaleimide in gel slices was quantified as previously described (Baird & Hammes, 1976).

RBL Cell Membrane Vesicle Preparation. The RBL cell subline 2H3 was maintained in cell culture, and plasma membrane vesicles were prepared from these cells following induction of membrane vesiculation of 50 mM formaldehyde with 1 mM dithiothreitol as described in the preceding paper (Holowka & Baird, 1983). Vesicles that had been dialyzed for 2 days against 10 mM sodium phosphate (pH 7.5), 0.1 M NaCl, and 0.01% sodium azide (PBS/NaN_3) containing protease inhibitors as described (Holowka & Baird, 1983) were stored at 4 °C and generally used within 1 week of preparation. Vesicle-bound receptors were saturated with IgE derivatives for energy-transfer measurements as follows. Typically 50–250 μL of a membrane vesicle suspension at a concentration of about 20 pmol of receptor/mL was incubated with a 2–3-fold molar excess of bindable IgE (as assessed by ability to bind to cells) for 2–4 h at 4 °C with periodic mixing. Nonbound IgE was separated from the vesicles by dilution of the suspension 10-fold with PBS/NaN_3 and then centrifugation at 25000*g* for 30 min (4 °C); supernatants were removed, and the membrane pellet was resuspended in 0.25–1.25 mL of PBS/NaN_3 as previously described (Holowka & Baird, 1983). Enumeration of bound IgE derivatives or amphipathic probes was done by measuring ^{125}I radioactivity or fluorescence of either the supernatant or pellet (or both) following this centrifugation procedure. Typically, 90–95% of the vesicles are recovered in the pellet with this procedure as determined by counting receptor-bound ^{125}I-IgE with a Beckman Gamma

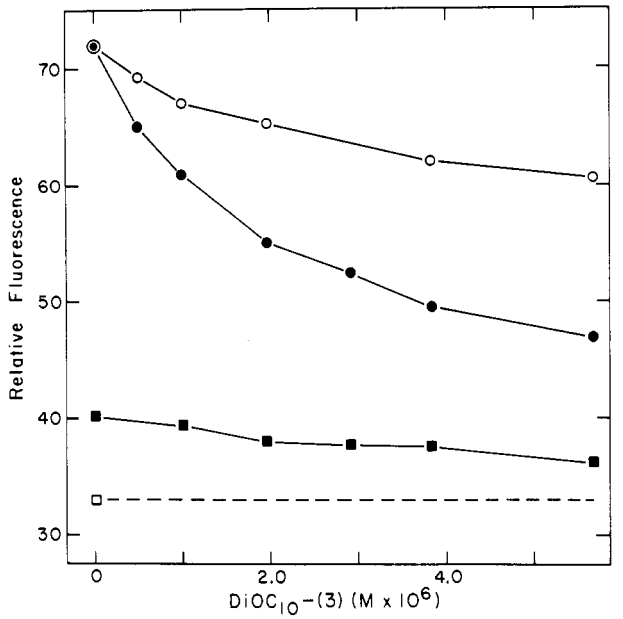

FIGURE 1: Fluorescence data (ex 395, em 470) from a representative experiment in which energy transfer was measured between CPM (donor) at the inter-ϵ disulfide of receptor-bound IgE and $DiOC_{10}$-(3) (acceptor) in the plane of the membrane bilayer as a function of acceptor concentration. The use of parallel samples A (●), B (○), and C (■) to calculate the efficiency of transfer is described in the text (Experimental Procedures). The level of light scattering from these samples is indicated (□).

4000. At the concentration of receptor employed for the fluorescence measurements (ca. 10 nM), essentially none of the IgE that is bound after this centrifugation step becomes dissociated during the remaining time of the experiment (Metzger et al., 1976).

Spectroscopic Measurements. General procedures used in making the absorption and fluorescence measurements are described in the preceding paper (Holowka & Baird, 1983). Except where indicated otherwise, energy-transfer measurements between donor probes on receptor-bound IgE and acceptor probes in the membrane vesicle bilayer were carried out by titrating a sample of vesicles containing bound IgE derivatives (in PBS/NaN_3 with protease inhibitors) with increasing concentrations of the amphipathic acceptor probe and observing the change in fluorescence intensity of the donor probe at a single emission wavelength (sample A). In order to correct for irrelevant changes in the fluorescence signal, two other samples also were titrated. One control sample (sample B) contained an equivalent quantity of vesicles but with receptors saturated by a 5–10-fold excess of *unmodified* IgE, and donor-labeled IgE (nonbound) was added such that the initial fluorescence was the same as that of sample A. This permitted the determination of any quenching of the donor probe due to direct interaction of the acceptor probe with IgE or the donor itself (see below). A second control sample (sample C) also contained an equivalent quantity of vesicles either without fluorescent IgE (when FITC was the donor) or with receptor-bound CPM–IgE(−) [when CPM–IgE(+) was the donor]. From sample C, the background signal and contributions from acceptor fluorescence were determined. The raw data from a representative experiment of this type is illustrated in Figure 1.

The efficiency of energy transfer (E) is given by

$$E = \frac{Q_D - Q_{DA}}{Q_D} \quad (1)$$

where Q_{DA} and Q_D are the donor fluorescence quantum yields in the presence and absence of acceptor, respectively. In our measurements, E was calculated from the equation

$$E = \frac{I^B - I^A}{I^B - I^C} \quad (2)$$

where I^A, I^B, and I^C are the intensities (fluorescence and scattered light) for the corresponding samples at the optimal excitation and emission wavelengths of the donor probe (see Figure 1). For the purposes of analysis, data were expressed as Q_D/Q_{DA}, which is obtained from eq 1 and 2:

$$\frac{Q_D}{Q_{DA}} = \frac{I^B - I^C}{I^A - I^C} \quad (3)$$

In these experiments, it is assumed that changes in the fluorescence intensity at a single wavelength reflect changes in the overall quantum yield of the donor (contributions of the acceptor's fluorescence preclude an examination of the entire donor emission spectrum). The critical transfer distance, R_0, for each donor–acceptor pair used (Table II)and the density in the plane of the membrane bilayer of acceptors HAE, ORB, and $DiOC_{10}$-(3) were determined as described in the preceding paper (Holowka & Baird, 1983). Measurement of the density of acceptor HAF was made by using 3-hexadecanoyl-7-hydroxycoumarin as donor; the R_0 for this donor–acceptor pair was determined to be 34.6 Å. For energy-transfer measurements using $DiOC_{10}$-(3) and ORB as acceptors, samples were incubated at 37 °C for 30 min to 1 h between fluorescence readings to accelerate the rate of insertion of these probes into the membrane bilayer.

Energy-Transfer Data Analysis. Distances of closest approach between fluorescent donors located at specific sites on the IgE molecules and energy acceptors randomly distributed along the membrane surface were obtained by fitting the experimental quenching profile (Q_D/Q_{DA} vs. acceptor density) to theoretical curves obtained with Monte Carlo calculations (Snyder & Freire, 1982). These calculations were carried out for the case of two infinite planes separated by a distance L: One plane contains a random distribution of donors and the other a random distribution of acceptors. Under these conditions, Q_D/Q_{DA} is given by

$$Q_D/Q_{DA} = N_D[\sum_{j=1}^{N_D}[1 + \sum_{k=1}^{N_A}(R_0/R_{D_jA_k})^6]^{-1}]^{-1} \quad (4)$$

where N_D and N_A are the number of donors and acceptors, respectively, the sum j is over all donors, the sum k is over all acceptors, and $R_{D_jA_k}$ is the distance between donor j and acceptor k. A set of theoretical curves Q_D/Q_{DA} vs. number of acceptors per R_0^2 were generated for different values of L/R_0. The experimental data for a given donor–acceptor pair were plotted in the same way, and the closest corresponding L/R_0 was determined by interpolation, by minimizing the root mean square deviation between the experimental curve and the series of theoretical curves.

Results

Modification of IgE with Fluorescent Probes. The reaction of IgE with FITC as described under Experimental Procedures results in the incorporation of 1.3–2.0 mol of FITC/mol of IgE. The absorption spectrum and corrected fluorescence emission spectrum of this derivative are shown in Figure 2A, and values for the quantum yield and steady-state fluorescence anisotropy are listed in Table II. When DNP-Lys is titrated into the anti-DNP combining sites of the FITC-modified IgE, significant quenching of the FITC fluorescence is observed (15–20% at saturation).[2] Since the R_0 for resonance energy

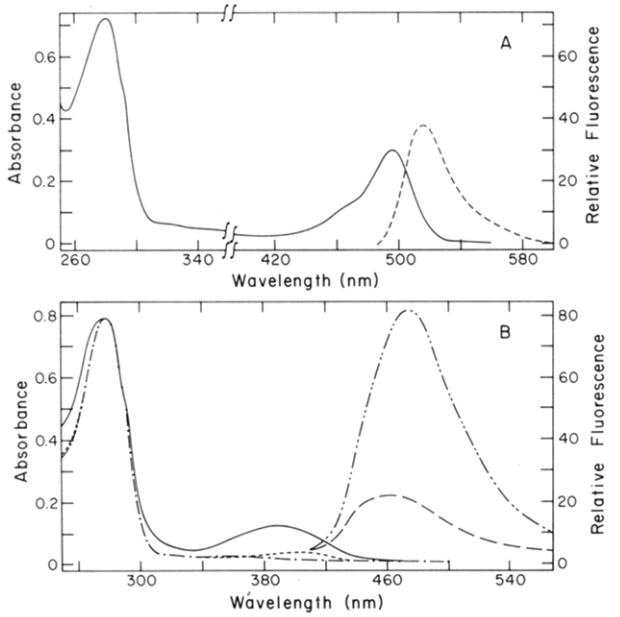

FIGURE 2: Absorption and corrected fluorescence emission spectra of fluorescent derivatives of IgE. (A) FITC–IgE: absorption spectrum in BBS, pH 8.0 (—); emission spectrum (excitation 480 nm) in PBS/NaN_3, pH 7.5 (---). (B) CPM–IgE derivatives: absorption spectra of CPM–IgE(+) (—), CPM–IgE(−) (---), and unmodified IgE (---) in BBS, pH 8.0; emission spectra (excitation 395 nm) of CPM–IgE(+) (-·--) and CPM–IgE(−) (--) in PBS/NaN_3, pH 7.5.

transfer between FITC as donor and DNP-Lys as acceptor is only 17 Å while the length of the native ϵ chain is probably at least 170 Å (by analogy with IgG; Amzel & Poljak, 1979), this observation suggests that FITC is not uniformly distributed over the whole IgE molecule.

Preferential labeling by FITC is further indicated by enzymatic digestion studies of FITC–IgE which show that a large fraction of this fluorescent label is located in the Fab segments of the IgE molecule. As shown in Figure 3A, lanes 1–6, digestion of FITC–IgE with DPCC-trypsin results in the generation of a fluorescent fragment with apparent M_r 52 000 which has been identified by Perez-Montfort & Metzger (1982) to be the first three domains of the mouse ϵ chain (V_H $C_\epsilon 1$ $C_\epsilon 2$). Quantitative analysis (see Experimental Procedures) showed this fragment to contain most of the FITC fluorescence; 23% of the fluorescence is contained in the light chain (κ; Liu et al., 1980) which is not digested significantly by DPCC-trypsin under these conditions. The remainder of the ϵ chain apparently is digested into small peptides which run at the electrophoretic front, and less than 10% of the total fluorescence is observed at this location until very long digestion times when the M_r 52 000 fragment breaks down (>6 h; data not shown). These results indicate that most of the FITC label is confined to the $F(ab')_2$ segment of IgE. Digestion of FITC–IgE by papain is shown in Figure 3B, lanes 1–6. At early time points the fluorescence appears in the intact ϵ and κ chains and in a fragment of the ϵ chain with apparent M_r 50 000 which appears to be similar to the fragment produced by the DPCC-trypsin digestion (V_H $C_\epsilon 1$ $C_\epsilon 2$). Longer times of papain digestion results in the generation of three new fluorescent bands: a band of apparent M_r 40 000, a band of apparent M_r 23 000, which may be the V_H $C_\epsilon 1$ fragment, and a band of apparent M_r 15 000, which is probably the V_H domain (Kocher & Spiegelberg, 1979). From these results it appears that most of the FITC label in FITC–IgE is present in the Fab segment (V_H $C_\epsilon 1$ and κ) rather than in the $C_\epsilon 2$–4 domains which apparently are digested to small fragments under these conditions (see below).

[2] A. Menon, J. Erickson, and D. Holowka, unpublished observations.

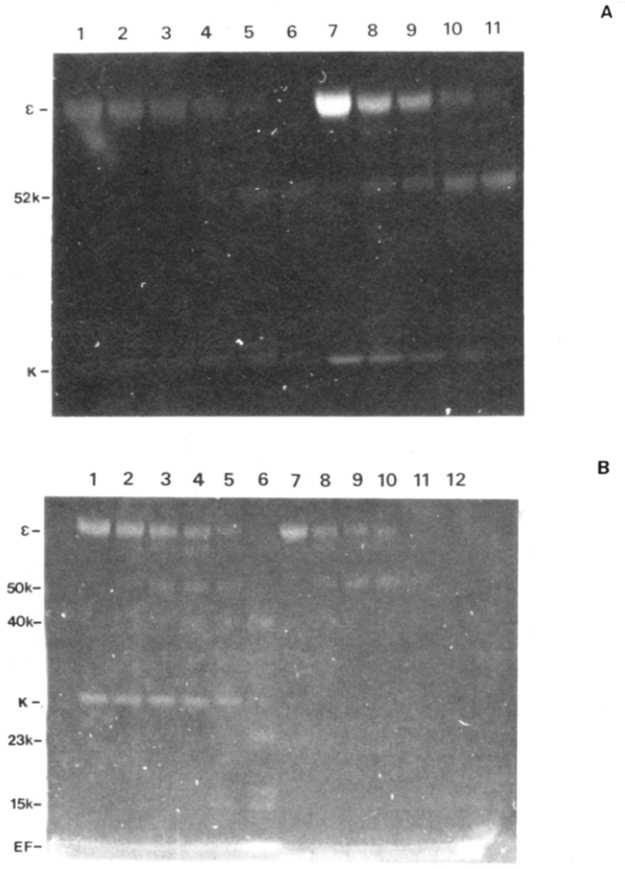

FIGURE 3: $NaDodSO_4$–polyacrylamide gel electrophoresis analysis of fluorescent products produced in the enzymatic digestion of IgE derivatives. (A) DPCC-trypsin digestion of FITC–IgE (lanes 1–6) and CPM–IgE(+) (lanes 7–11). Digestion times are as follows: lanes 1 and 7, 0 min; lanes 2 and 8, 10 min; lanes 3 and 9, 60 min; lanes 4 and 10, 180 min; lanes 5 and 11, 360 min; lane 6, 1500 min. (B) Papain digestion of FITC–IgE (lanes 1–6) and CPM–IgE(+) (lanes 7–12). Digestion times are as follows: lanes 1 and 7, 0 min; lanes 2 and 8, 20 min; lanes 3 and 9, 70 min; lanes 4 and 10, 135 min; lanes 5 and 11, 280 min; lanes 6 and 12, 1320 min. 11% acrylamide (w/v) was used in (A), and 12.5% (w/v) in (B). Each lane was loaded with 15 μg of digested IgE. The numbers on the left-hand margin indicate the apparent molecular weight (×10^3); EF indicates the electrophoretic front.

In order to place probes at defined sites in the IgE molecule, the strategy of selective reduction and alkylation of disulfide bonds was employed. Preliminary studies were carried out with dithiothreitol (1 mM) as the reducing agent and [^{3}H]-*N*-ethylmaleimide (2.5 mM) as the alkylating agent. Under the conditions described under Experimental Procedures, 2–3 mol of [^{3}H]-*N*-ethylmaleimide are incorporated per mol of IgE, and the distribution of ^{3}H label in the resulting IgE polypeptides as determined by $NaDodSO_4$–polyacrylamide gel electrophoresis under nonreducing conditions is summarized in Table I. The ϵκ half-molecule, identified according to molecular weight, contained the largest fraction of [^{3}H]-*N*-ethylmaleimide, and about 40% of the total Coomassie blue stained IgE was in this band as evaluated by visual inspection (not shown). Importantly, no stained band could be detected in the region expected for the κ chain, and only a trace of the free ϵ chain could be seen (4 μg of IgE was loaded on the gel). These results indicate that the inter ϵ chain disulfide bonds are more susceptible to reductive cleavage than the inter-ϵ–κ bonds in mouse IgE and that more than one disulfide bond probably must be cleaved to generate ϵκ half-molecules.

Table I: Summary of IgE Labeling by Reduction and Alkylation[a]

derivative	mol of *N*-ethylmaleimide or CPM/mol of IgE	reduced gels[b]	NaDodSO$_4$-PAGE:[c] distribution of label in IgE (%) $\epsilon_2\kappa_2$	$\epsilon\kappa$	ϵ	κ
[^{3}H]-*N*-ethylmaleimide-IgE (1 mM dithiothreitol)	2.89	−	20	69	11	
CPM-IgE(+) (1 mM dithiothreitol)	1.08[d]	−	58	40	0	2
		+	0	0	97	3
CPM-IgE(−) (no dithiothreitol)	0.23	−	100	0	0	0
		+	0	0	100	0

[a] Reactions and quantitative analysis carried out as described under Experimental Procedures. [b] Complete reduction of samples with β-mercaptoethanol immediately prior to NaDodSO$_4$-polyacrylamide gel electrophoresis. [c] NaDodSO$_4$-PAGE, sodium dodecyl sulfate-polyacrylamide gel electrophoresis. [d] From absorption spectrum (Figure 1) after correction for unbound CPM (17% of total) as determined from fraction of total CPM fluorescence on NaDodSO$_4$-polyacrylamide gel electrophoresis which ran at the dye front.

Table II: Summary of Energy-Transfer Measurements

donor	Q_D	$\bar{A}$[a]	acceptor	R_0 (Å)	L (Å)
FITC-IgE	0.41	0.19	HAE	53.0	86
FITC-IgE	0.41	0.19	ORB	53.2	91
CPM-IgE(+)	0.36	0.23	$DiOC_{10}$-(3)	51.7	43[b,c]
CPM-IgE(+)	0.36	0.23	HAF	47.4	44[b,d]
CPM-IgE(−)	0.58	0.29			

[a] Steady-state anisotropy measured at the wavelengths of maximum excitation and emission. [b] These distances pertain to CPM at inter-ϵ disulfides and acceptor probes at membrane surface, calculated as described in text. [c] Data from Figure 5 used for analysis excluded the point at the highest value of αR_0^2 (0.74). [d] Data from Figure 6 used for analysis excluded the two points at the highest values of αR_0^2 (0.90 and 1.03; see text).

Alkylation of dithiothreitol-reduced IgE with 3 mM CPM to prepare CPM–IgE(+) under the same conditions as those for [^{3}H]-*N*-ethylmaleimide results in somewhat less labeling (Table I), probably due to the poor solubility of CPM in aqueous solution. Alkylation of IgE with CPM without prior reduction [CPM–IgE(−)] results in the incorporation of a substantially lower amount of CPM than in CPM–IgE(+) (Table I), and the absorption spectra and corrected emission spectra of these two derivatives are somewhat different, as indicated in Figure 2B. Prealkylation of IgE with 3 mM *N*-ethylmaleimide does not reduce the amount of CPM that is subsequently incorporated in the absence of reduction, and this along with the altered spectral properties suggests that a site other than a sulfhydryl group is being modified to a small extent. The quantum yield of CPM–IgE(+) is somewhat lower than that of CPM–IgE(−) (Table II), probably due in part to stacking interactions between CPM fluorophores at adjacent –SH groups in the former derivative. NaDodSO$_4$–polyacrylamide gel electrophoresis under nonreducing conditions reveals that for CPM–IgE(+), about 40% of the protein-bound coumarin fluorescence is found in the $\epsilon\kappa$ half-molecule and less than 5% is seen in either the free ϵ or κ chains (Table I). Some significant fluorescence is seen at the electrophoretic front of this derivative (Table I), probably due to the difficulty of removing insoluble CPM–dithiothreitol conjugates (see Experimental Procedures). This product is not seen in the CPM–IgE(−) derivative, and all of the label is confined to the ϵ chain as visualized after NaDodSO$_4$–polyacrylamide gel electrophoresis under reducing conditions (not shown).

Digestion of CPM–IgE(+) with DPCC-trypsin reveals that, as with FITC–IgE, a large fraction of the fluorescence is associated with the 52 000-dalton ϵ fragment which is comprised of the V_H $C_\epsilon1$ $C_\epsilon2$ domains (Figure 3A, lanes 7–11). Several other minor labeled bands can be seen, including the κ chain. In this preparation the κ chain contained a larger fraction of CPM (10%) than in those preparations employed in other experiments described in this report (Tables I and II; Figures 3B and 6), probably because somewhat more reduction had occurred during the modification procedure. The fluorescence in the κ band appears to decrease gradually during the digestion time course, although the Coomassie blue staining pattern showed that the amount of protein in this band did not decrease significantly as was observed for the FITC–IgE (data not shown). The fluorescence in the ϵ chain is rapidly reduced within the first hour of digestion (compare lane 7 with lane 8 in Figure 3A), and this corresponds to the measured increase in the amount of CPM fluorescence at the electrophoretic front (~33% increase in fluorescence from the t = 0 value). Subsequent time points (60–360 min) show a slow first-order decrease in the labeled ϵ band which corresponds to the appearance of the M_r 52 000 band described above; the CPM fluorescence at the front was measured and found to remain constant during this time. These results suggest that a fraction of the IgE has been denatured during the reaction with CPM and these molecules are rapidly degraded to small peptides by the trypsin; the nondenatured CPM–IgE is digested to yield the F(ab′)$_2$ fragments seen by Perez-Montfort & Metzger (1982) which contain the CPM fluorescence. Since there is no increase in fluorescence at the electrophoretic front during the time that the F(ab′)$_2$ fragments are being generated, we conclude that the CPM label is located primarily in this portion of the intact IgE molecules. Furthermore it is highly likely that only nondenatured CPM–IgE(+) binds to membrane receptors in the energy-transfer experiments (see below).

Digestion of CPM–IgE(+) with papain has a Coomassie blue stained protein fragmentation pattern identical with that seen with FITC–IgE (not shown), but the distribution of the fluorescence in the fragments is notably different. As shown in Figure 3B the initial digestion of CPM–IgE(+) results in most of the fluorscent label migrating with the 50 000-dalton fragment seen also with the FITC–IgE. However, unlike the FITC–IgE, further digestion of CPM–IgE results in the disappearance of fluorescent bands except for very low molecular weight products which run at the front. Digestion fragments corresponding to the fluorescent bands seen for FITC–IgE in Figure 3B, lane 6, are stained by Coomassie blue for CPM–IgE (not shown) but contain no fluorescence (Figure 3B, lane 12). We conclude from these results that most of the CPM fluorescence seen in the V_ϵ $C_\epsilon1$ $C_\epsilon2$ fragment of CPM–IgE(+) (stable product of DPCC-trypsin and transient product of papain) is confined to the $C_\epsilon2$ domains, which is ultimately digested into small peptides by papain.

Energy-Transfer Measurements. For these experiments FITC–IgE or CPM–IgE contained the fluorescent donor probes at the sites characterized above. The acceptor probes

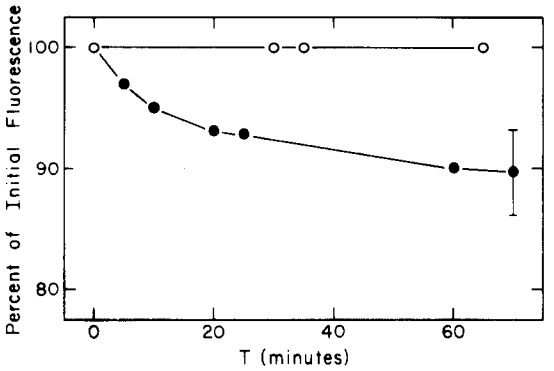

FIGURE 4: Fluorescence quenching of FITC–IgE accompanying binding to receptors on membrane vesicles containing membrane-bound HAE. The FITC–IgE (2.7 pmol) was added to suspensions of vesicles (5.4 pmol of receptor) in PBS, pH 7.5, which either had HAE (1.3×10^{-4} acceptors/Å^2) (●) or did not have HAE (○), and fluorescence (ex 480 nm, em 510 nm) was followed with time. Background signal due to light scattering has been subtracted.

were on amphipathic molecules which have been shown to insert and distribute randomly in the bilayer plane of plasma membrane vesicles isolated from RBL cells (Holowka & Baird, 1983). In the experiment shown in Figure 4 a sample of the isolated vesicles was divided into two, and only one portion was incubated with the amphipathic acceptor probe HAE prior to the final centrifugation and resuspension. FITC–IgE was then added to both samples under conditions of receptor molar excess, and changes in the donor FITC fluorescence after initial mixing were monitored with time. As can be seen in Figure 4, significant quenching of the FITC fluorescence occurs only in the sample containing HAE, and the time course of this quenching is consistent with the kinetics of IgE binding to membrane-bound receptor under these conditions (Metzger et al., 1976). After 70 min of incubation, 10.3 ± 3.5% of the control FITC fluorescence is quenched, and this corresponds to a transfer efficiency $E = 0.14 \pm 0.05$ when the fraction of IgE that has become bound after this time is taken into account.

To alleviate the problems of low signal to noise ratio and the necessity of determining the fraction of IgE bound in these experiments, furthur energy-transfer measurements were carried out by prebinding fluorescent IgE derivatives to receptors on the vesicles. Then the amphipathic acceptor probes were titrated into the vesicle bilayer, and the donor fluorescence was monitored as a function of acceptor density. In one set of experiments vesicles were prepared from cells that had had receptors saturated with FITC–IgE, and vesicles with receptors saturated with unlabeled IgE were prepared in parallel for control samples. As described in the preceding paper (Holowka & Baird, 1983), essentially all (>98%) of the IgE recovered with the membranes under these conditions is receptor bound. Fluorescence excitation and emission spectra of the membrane-bound FITC–IgE derivative were found to be indistinguishable from those for the soluble FITC–IgE (Figure 2A). The amphipathic acceptor probe HAE was titrated into the membrane vesicle preparations, and simultaneous quenching of the receptor-bound FITC–IgE fluorescence was observed. As described under Experimental Procedures, irrelevant changes in the fluorescence were monitored by performing a similar titration in a parallel sample that contained membrane vesicles with receptors occupied by unlabeled IgE, and FITC–IgE was present in solution. The density of HAE in the plane of the membrane bilayer (σ, acceptors per Å^2) was determined for each addition by measuring the efficiency of energy transfer between HAF and

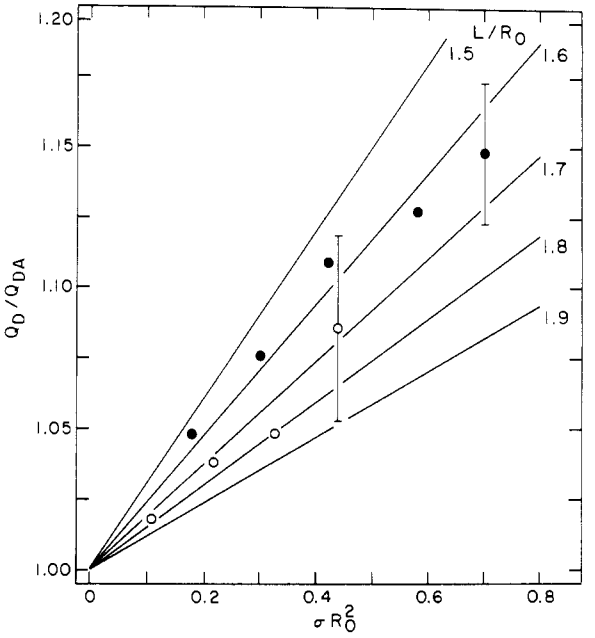

FIGURE 5: Energy transfer between receptor-bound FITC–IgE and acceptors at the membrane surface. The ratio of donor quantum yield in the absence (Q_D) and presence (Q_{DA}) of acceptors [HAE (●); ORB (○)] is plotted as a function of acceptor density (acceptors/R_0^2). The representative error bars were calculated from a propagation of error analysis of eq 3. The curves are calculated from eq 5 for different values of L/R_0.

HAE in a separate aliquot of vesicles as previously described (Holowka & Baird, 1983). The results from an experiment of this design are shown in Figure 5 (open circles), where the ratio of donor (FITC–IgE) fluorescence quantum yield in the absence (Q_D) and in the presence (Q_{DA}) of HAE is plotted as a function of σR_0^2.

A similar measurement was made with FITC–IgE by using ORB as the membrane surface energy-transfer acceptor. In this experiment, vesicles prepared in the absence of IgE were incubated with a 2-fold molar excess of bindable FITC–IgE (the preparation was 75% bindable) and then washed by pelleting and resuspension as described under Experimental Procedures. When an equal amount of ^{125}I-IgE was included in the wash step, it was determined that >95% of the FITC–IgE remaining associated with the vesicles was receptor bound. The results from the titration of these vesicles with ORB are shown in Figure 5 (filled circles). It can be seen that the fluorescence of receptor-bound FITC–IgE is quenched to a similarly low extent by both surface acceptors, HAE and ORB. Furthermore, when compared at the same acceptor density, the amount of energy transfer observed in these experiments agrees with the results of the experiment shown in Figure 4 which was carried out with a different protocol. The data shown in Figure 5 were analyzed in terms of eq 4 by using the Monte Carlo method of Snyder & Freire (1982). The results of this analysis which are summarized in Table II give the distance (L) between the FITC label that is located primarily in the Fab segments of receptor-bound IgE and acceptor probes at the membrane surface to be 85–90 Å (assuming two parallel planes).

For energy-transfer measurements with CPM–IgE as donor, 2-fold molar excess amounts of bindable CPM–IgE(+) and CPM–IgE(−) derivatives were incubated with samples of vesicles in parallel and washed in the manner described above with FITC–IgE. The CPM–IgE preparations had lower binding activity (30–40% bindable for both), probably due to some denaturation during the modification reaction. Under

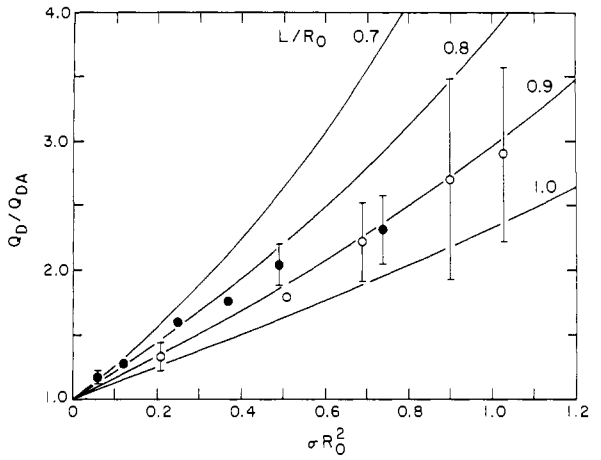

FIGURE 6: Energy transfer between receptor-bound CPM–IgE and acceptors at the membrane surface. [For these measurements the fluorescence of CPM–IgE(+) was corrected by subtraction of the signal from that of CPM–IgE(−) as described in text.] The ratio of donor quantum yield in the absence (Q_D) and presence (Q_{DA}) of acceptors [DiOC$_{10}$-(3) (●); HAF (○)] is plotted as a function of acceptor density (acceptors/R_0^2). The error bars and the curves were calculated as described in Figure 5.

these conditions, ≥90% of the CPM–IgE associated with the washed vesicles was receptor bound. The fluorescence emission spectra of the membrane-bound derivatives were identical with those obtained in solution (Figure 2B), and the ratio of the fluorescence intensity at 470 nm (ex 395 nm) for equal quantities of membrane-bound CPM–IgE(+) vs. membrane-bound CPM–IgE(−) was 4.5 ± 0.4 for three different experiments. This value compares to that of 3.8 for these same derivatives in solution and indicates that IgE molecules which have been reduced and alkylated at their inter-ε disulfide bonds bind to receptor at least as well as unreduced molecules. Consistent with this is an observation made in preliminary experiments with IgE that was reduced in the same way and then alkylated with IAEDANS. Incubation of this derivative with whole cells and analysis of the receptor-bound material on NaDodSO$_4$–polyacrylamide gel electrophoresis without further reduction clearly showed the presence of fluorescent εκ half-molecules (data not shown).

As described above, CPM–IgE(+) probably contains most of the fluorescent label in the C$_ε$2 domain at the location of the inter-ε disulfide bonds. In order to determine the distance between this region on receptor-bound IgE and the membrane surface, the CPM–IgE(+) bound to vesicles was titrated with two different amphipathic acceptor probes, HAF and DiOC$_{10}$-(3), and a set of fluorescence measurements was carried out for each of these as described above for FITC–IgE. In addition, a vesicle sample with bound CPM–IgE(−) also was titrated with acceptor in order to correct for contribution to the fluorescence from CPM at the non-sulfhydryl site (sample C). Data from these experiments were analyzed as described under Experimental Procedures, and the plots of Q_D/Q_{DA} vs. σR_0^2 are shown in Figure 6. It can be seen that the fluorescence quenching of membrane-bound CPM–IgE is similar for both acceptors, HAF and DiOC$_{10}$-(3). This quenching is significantly greater than that seen with membrane-bound FITC–IgE for the same densities of acceptors (Figure 5). Values for L/R_0 were obtained by the fitting procedures described above, and the results are summarized in Table II. The calculated value for L, the distance of closest approach between donor CPM at the inter-ε sulfhydryl groups and acceptor probes at the membrane surface (assuming two parallel planes), is in the range 40–45 Å for both acceptors employed. This distance is substantially less than that obtained with FITC–IgE, where the donor probe is located primarily in the Fab segments.

Discussion

In this report we have demonstrated the utility of resonance energy-transfer methods for probing structural details of the membrane-associated IgE–receptor complex. Our approach has capitalized on the ability to label isolated IgE with donor probes and on the very tight association between IgE and its cell surface receptor. With the methods described similar studies with other cell surface receptors also should be possible by using donor-labeled ligand or monoclonal Fab fragments that are specific for a particular surface component.

In order to properly interpret the results obtained with the fluorescence measurements in our system, the specificities of the chemical modifications must be assessed. As shown in the previous report amphipathic acceptors distribute randomly in the plane of the membrane bilayer of the vesicles, and the average density of the probes can be determined spectroscopically (Holowka & Baird, 1983). For FITC–IgE, the DNP-lysine titration results and the proteolytic digestion studies taken togethere indicate that a large fraction of the donor probe FITC that is conjugated to IgE is located in the Fab segments. It is possible that there is an especially reactive residue in this region of the molecule; precedence for selective modification of proteins by FITC exists (Carilli et al., 1982; Pick & Karlish, 1980). Although it is likely that some FITC modification also has occurred in the F$_c$ segment, NaDodSO$_4$–polyacrylamide gel electrophoresis shows that this accounts for less than 10% of the label present. The relative quantum yields of FITC at different sites on IgE are unknown; however, above pH 7.0 fluorescein is generally not extremely sensitive to microenvironment.

The procedures used to prepare CPM–IgE(+) involve mild reduction of mouse IgE with 1 mM dithiothreitol which appears to selectively reduce inter-ε disulfide bonds such that some εκ half-molecules are generated following alkylation and denaturation in NaDodSO$_4$. These results contrast markedly to those obtained with human IgE; in that case only the inter-light-ε chain disulfide bonds are susceptible to reductive cleavage with 1 mM dithiothreitol, an intra-ε disulfide in C$_ε$1 also is cleaved with 2 mM DTT, and one or both of the inter-ε disulfide bonds also are cleaved with 10 mM DTT (Takatsu et al., 1975; Dorrington & Bennich, 1978). Furthermore we find that, unlike human IgE, complete reduction of the inter-ε disulfide bonds on mouse IgE does not prevent binding to the receptor. Consistent with our observations is the report that reduction of rat IgE with 5 mM DTT does not appreciably reduce its ability to bind to receptor from RBL cells (Perez-Montfort & Metzger, 1982).

Recent DNA sequence analysis of the gene coding for the mouse ε polypeptide has revealed a number of differences from the human ε polypeptide, including the absence of a second intrachain disulfide in mouse C$_ε$1 (Ishida et al., 1982) and the presence of a third cysteine residue in C$_ε$2 (Ishida et al., 1982; Liu et al., 1982). Since two to three interchain disulfides appear to be present in the mouse C$_ε$2 domain, most of the CPM label must be present there in order to account for the yield of εκ half-molecules that we obtained with partial reduction and alkylation. This is consistent with our enzymatic digestion studies and the interpretation that papain digestion results in the conversion of V$_H$ C$_ε$1 C$_ε$2 fragments [F(ab′)$_2$] to unlabeled V$_H$ C$_ε$1 fragments and small labeled C$_ε$2 peptides. The interpretation of the energy-transfer data discussed below is based on our conclusion that essentially all of the CPM

donor probe is confined to the $F(ab')_2$ segment and that most of it is located in the $C_\epsilon 2$ domain.

In our fluorescence measurements it is clear that FITC located primarily in the Fab region of receptor-bound IgE is quenched significantly less than CPM, located in the $C_\epsilon 2$ domains, when spectrally appropriate amphipathic acceptor probes are titrated into the membrane bilayer. Although this quenching could occur through more than one mechanism, the contribution due to resonance energy transfer can be assessed. As shown for FITC–IgE and HAE in Figure 4, if the acceptor is already present in the vesicles when donor-labeled IgE is added, the fluorescence quenching follows the kinetics of IgE binding which indicates that the quenching observed is due to energy transfer from donors on bound IgE. In experiments where the acceptor was titrated into sample of vesicles containing bound IgE, it was observed that some apparent collisional quenching also occurs. This probably is due to a weak interaction of the amphipathic acceptor probe with a site on IgE or with the donor probe itself. Therefore we designed our experiments such that these contributions could be detected and corrected for by carrying out the same titration in a sample in which donor-labeled IgE is present but not receptor bound (Figure 1). This irrelevant quenching varies with donor and acceptor probes and, for instance, is less with FITC–IgE and ORB or HAE than for CPM–IgE(+) and $DiOC_{10}$-(3) (Figure 1); this contribution is greater with CPM–IgE(+) and HAF, making the last two points in that titration curve (Figure 5) subject to a high degree of uncertainty. The physical basis for this rather marked tendency of some amphipathic probes to interact with protein-bound donor probes is not known, but our observations point out the necessity of accounting for these effects when data of this type are analyzed. The possibility also exists that the acceptor probes change the quantum yield of the donor by a conformational effect, but although we cannot rule this out rigorously, we think it unlikely because similar distance determinations (L) were obtained with two different acceptor probes of opposite charge for each of the donor–IgE derivatives (Table II).

For interpretation of the energy-transfer data in terms of distances, R_0 was calculated for each donor–acceptor pair assuming the orientation factor, κ^2, is $^2/_3$ which corresponds to the case where the probes rotate rapidly relative to the fluorescence lifetime of the donor. As listed in Table II, the steady-state anisotropy values for FITC–IgE and CPM–IgE-(+) are indicative of some limited angular rotation of the donor emission dipole(s), and a distribution of acceptor dipoles also is expected (Holowka & Baird, 1983), so the probability of finding an extreme situation of donor–acceptor dipole alignment is unlikely (Stryer, 1978; Fung & Stryer, 1978). The agreement seen in Table II for values of L using different acceptor probes with the same donor supports this conclusion.

The model employed in analyzing the energy-transfer results assumes that the distribution of donors is confined to a plane at some fixed distance away from the plane of acceptor chromophores at the membrane surface. In the cases considered here, this is clearly an approximation, but it provides an "average" distance for comparison. The effect of more than one donor plane on the calculated distance can be assessed by using a linear approximation valid in the limit of low energy transfer. For a single donor and a single acceptor plane this is given by eq 5 (Dewey & Hammes, 1980; Shaklai et al., 1977):

$$\frac{Q_D}{Q_{DA}} = 1 + \frac{\pi R_0^6 \sigma}{2}\left(\frac{1}{L}\right)^4 \qquad (5)$$

In this limit it easily can be shown (see Appendix) that for n planes containing equal numbers of donors and a single acceptor plane eq 5 may be generalized as

$$\frac{Q_D}{Q_{DA}} = 1 + \frac{\pi R_0^6 \sigma}{2n}\sum_{j=1}^{n}\left(\frac{1}{L_j}\right)^4 \qquad (6)$$

It can be seen that the distance to the jth plane is averaged according to $(1/n)(1/L_j)^4$, and therefore the closer planes are weighted more heavily. For FITC–IgE there may be several planes of donors including a small fraction (~10%) in the F_c region. If the F_c region is closer to the membrane than the Fab regions, this means that the values listed in Table II underestimate the distance from probes located in the Fab region. For CPM–IgE(+), there are likely to be at least two planes of donor, one for each disulfide bond in $C_\epsilon 2$. In the absence of any information as to the relative rates of labeling of these two disulfide bonds, and the relative quantum yields of the probes at these sites, we cannot assign a precise site-to-surface distance. If the assumption is made that both of these sites are equally labeled by CPM and separated by ~40 Å at either end of the $C_\epsilon 2$ domain, then analysis of the data according to eq 6 indicates that the closer site would have an L value about 15% smaller than those given in Table II. The assumption that all of the acceptor probe is distributed on the outer half of the membrane bilayer may be questioned, as discussed previously (Holowka & Baird, 1983); however, this would cause little error in these distance calculations because acceptors present on the inside half of the bilayer would be too far away from donors (>80 Å) to contribute very significantly to the energy-transfer process. From a simple analysis of the propagation of error in the experimental data, we can assign limits of about ±20% to the values of L listed in Table II.

Despite the uncertainties discussed above, the values of L given in Table II put some constraints upon the possible orientations of the receptor-bound IgE with respect to the membrane surface. FITC in the Fab segments is at least 45 Å further away from the membrane surface than is CPM in the $C_\epsilon 2$ domains, indicating that the antibody combining sites extend outward in some way from the membrane receptor which binds the F_c region. Further support of this has come from recent energy-transfer experiments where we determined that the distance between dansyllysine in the anti-dansyl combining sites of receptor-bound monoclonal IgE and the membrane surface is greater than 100 Å.[3] These results specifically indicate that the long axes of the Fab′ segments are not oriented parallel to the membrane. The CPM label in the $(C_\epsilon 2)_2$ region of receptor-bound IgG is only 35–52 Å from the membrane surface (numbers allow for 20% error). This means that the $(C_\epsilon 3\ C_\epsilon 4)_2$ domains of IgE cannot be fully extended and oriented perpendicular to the membrane surface with the C terminus at the surface, because in that case the distance between the surface and the closest part of the $C_\epsilon 2$ domain would be the length of two domains, about 70–80 Å. Several other alternatives are possible. The distances obtained in our experiments would allow a structural arrangement where the C-terminal end of the bound IgE molecule is buried about 40 Å beneath the membrane surface; however, evidence from other recent experiments suggests this is unlikely as follows: The membrane integral β subunit of the receptor is not required for IgE binding to α (Holowka & Metzger, 1982), while the α subunit does not seem to require detergents for solubility[4]

[3] D. Holowka and B. Baird, unpublished experiments.

and thus may not interact appreciably with the hydrocarbon core of the lipid bilayer. Also the F_c region of IgE is susceptible to enzymatic digestion when bound to α in purified IgE–α complexes (Perez-Montfort & Metzger, 1982). Furthermore, studies with a monoclonal antibody specific for the $(C_\epsilon 3\ C_\epsilon 4)_2$ domains of rat F_c show that the antigenic site is completely accessible on cell-bound IgE (Conrad et al., 1983).

A simple model consistent with our current results and other published information is one in which the C-terminal end of receptor-bound IgE is near the membrane surface and the length of the molecule is disposed at an angle to the surface with the $C_\epsilon 2$ domains and the Fab segments at the distances indicated. Another possibility is that the bound IgE molecule is bent near its point of attachment to the receptor α subunit (which may itself protrude some distance from the membrane surface). In an extreme variation of this model, bound IgE would form a right angle with the longitudinal (2-fold) axis of symmetry of the $F(ab')_2$ segment oriented perpendicular to the long axis of $(C_\epsilon 3\ C_\epsilon 4)_2$ and to the plane of the membrane surface. Both of these models are consistent with the known molecular properties of the IgE–receptor interaction including the suggestion that the binding to receptor occurs with some portion of the $C_\epsilon 3$ domain (see the introduction). IgE in solution appears to exhibit some restricted segmental flexibility (Cathou, 1978), and by analogy with the sites of flexibility in IgM (Holowka & Cathou, 1976), IgE could also bend at the $C_\epsilon 2$–$C_\epsilon 3$ interface. In light of this possible flexibility these two models may not really be distinct, although the binding process might impose some rigidity in the structure of IgE. The experimental system described in this report can now be used to distinguish among these possibilities and also address other questions regarding the structure of the membrane-bound IgE–receptor complex.

Acknowledgments

We are grateful to Dr. Brian Snyder for carrying out the Monte Carlo calculations and to Professor Gordon G. Hammes for helpful discussions.

Appendix

Energy Transfer between n Planes of Donors and a Single Plane of Acceptors. We treat the case where all planes are infinite and parallel, and the jth donor plane is a distance L_j from the acceptor plane which contains a uniform density of acceptor molecules, σ (acceptors per Å^2). It is assumed the same R_0 exists for all donor–acceptor pairs. We consider only the situation of low extent of energy transfer where simplifying approximations can be made. (In our experiments this situation corresponds to the initial linear portion of the acceptor titration curves seen in Figures 5 and 6.) Our treatment is a simple extension of the derivations carried out by Shaklai et al. (1977) and Hammes (1981).

The rate equation for an excited donor in the jth plane, D_j^*, can be written as

$$\frac{d(D_j^*)}{dt} = R - (k_f + k_c + k_{t_j})(D_j^*)$$

where R is the rate of production of the excited state and k_f and k_c are the rate constants for fluorescence and internal conversion, respectively; these values are assumed to be the same for all donors in all planes. The parameter k_{t_j} is the rate constant for energy transfer from a single donor in the jth plane to all of the acceptors in the acceptor plane. In the steady state $d(D_j^*)/dt = 0$ and $(D_j^*) = R(k_f + k_c + k_{t_j})^{-1}$ for each donor. Let a_j/n be the fraction of total donor molecules that are in the jth plane such that a_j is the relative number of donor molecules in the jth plane, and $\sum_{j=1}^{n} a_j = n$. The observed fluorescence is the sum of the fluorescence emitted from all donors and is proportional to

$$k_f \sum_{j=1}^{n} a_j(D_j^*) = Rk_f \sum_{j=1}^{n} a_j(k_f + k_c + k_{t_j})^{-1} = R\sum_{j=1}^{n} a_j Q_j$$

The quantum yield, Q_j is defined as $Q_j = k_f(k_f + k_c + k_{t_j})^{-1}$. When no acceptors are present $\sigma = 0$ and $k_{t_j} = 0$, and the observed fluorescence is proportional to

$$Q_D = \sum_{j=1}^{n} a_j(Q_D)_j = nk_f(k_f + k_c)^{-1}$$

When acceptors are present, the observed fluorescence is proportional to

$$Q_{DA} = \sum_{j=1}^{n} a_j(Q_{DA})_j = \sum_{j=1}^{n} a_j k_f(k_f + k_c + k_{t_j})^{-1}$$

Then

$$\frac{Q_{DA}}{Q_D} = \frac{1}{n}\sum_{j=1}^{n} a_j \left(1 + \frac{k_{t_j}}{k_f + k_c}\right)^{-1} \tag{A1}$$

This equation is general for any amount of energy transfer.

In the case of low extent of energy transfer k_{t_j} can be approximated as (Shaklai et al., 1977)

$$k_{t_j} \approx \int_{L_j}^{\infty} \sigma(k_f + k_c)\left(\frac{R_0}{R}\right)^6 2\pi R\, dR = \frac{\pi R_0^6 \sigma(k_f + k_c)}{2L_j^4}$$

Substitution into eq A1 yields

$$\frac{Q_{DA}}{Q_D} = \frac{1}{n}\sum_{j=1}^{n} a_j \left(1 + \frac{\pi R_0^6 \sigma}{2L_j^4}\right)^{-1}$$

Under conditions corresponding to low energy transfer k_{t_j} is small allowing a truncated series approximation $[(1 + x)^n \approx 1 + nx]$ to yield

$$\frac{Q_{DA}}{Q_D} = \frac{1}{n}\sum_{j=1}^{n} a_j \left(1 - \frac{\pi R_0^6}{2L_j^4}\sigma\right) = 1 - \frac{\pi R_0^6 \sigma}{2n}\sum_{j=1}^{n}\frac{a_j}{L_j^4}$$

This equation provides a useful linear relationship between Q_{DA}/Q_D and σ; however, for comparison to our other analysis (Figures 5 and 6) both sides of the equation are inverted, and then, with the condition of low energy transfer, the right hand side is approximated with a truncated series expansion to yield

$$\frac{Q_D}{Q_{DA}} = 1 + \frac{\pi R_0^6 \sigma}{2n}\left(\sum_{j=1}^{n}\frac{a_j}{L_j^4}\right)$$

This equation is a generalization of the linear relationship between Q_D/Q_{DA} that has been derived for a single donor plane ($n = 1$) (Shaklai et al., 1977; Dewey & Hammes, 1980). In the general case it can be seen that the slope of the line is weighted according to $(a_j/n)(1/L_j)^4$ for each donor plane. When the donor planes are equally labeled, $a_j = 1$.

[4] H. Metzger and associates, personal communication.

Registry No. HAF, 73024-80-3; ORB, 65603-19-2; FITC, 3326-32-7; CPM, 76877-33-3; IAEDANS, 36930-63-9; $DiOC_{10}$-(3), 68006-77-9.

References

Amzel, L. M., & Poljak, R. J. (1979) *Annu. Rev. Biochem. 48*, 961–997.

Baird, B. A., & Hammes, G. G. (1976) *J. Biol. Chem. 251*, 6953–6962.

Carilli, C. T., Farley, R. A., Perlman, D. M., & Cantley, L. C. (1982) *J. Biol. Chem. 257*, 5601–5606.

Cathou, R. E. (1978) *Compr. Immunol. 5*, 37–83.

Conrad, D. H., & Froese, A. (1976) *J. Immunol. 116*, 319–326.

Conrad, D. H., Studer, E., & Mohanakumar, T. (1983) *Int. Arch. Allergy Appl. Immunol.* (in press).

Dewey, T. G., & Hammes, G. G. (1980) *Biophys. J. 32*, 1023–1036.

Dorrington, K. J., & Bennich, H. H. (1978) *Immunol. Rev. 41*, 3–25.

Fung, B. K.-K., & Stryer, L. (1978) *Biochemistry 17*, 5241–5248.

Hammes, G. G. (1981) in *Protein-Protein Interactions* (Frieden, C., & Nichol, L. W., Eds.) pp 257–287, Wiley-Interscience, New York.

Holowka, D. A., & Cathou, R. E. (1976) *Biochemistry 15*, 3379–3390.

Holowka, D., & Metzger, H. (1982) *Mol. Immunol. 19*, 219–227.

Holowka, D., & Baird, B. (1983) *Biochemistry* (preceding paper in this issue).

Holowka, D., Hartman, H., Kanellopoulos, J., & Metzger, H. (1980) *J. Recept. Res. 1*, 41–68.

Ishida, N., Veda, S., Hayashida, H., Miyata, T., & Honjo, T. (1982) *EMBO J. 1*, 1117–1123.

Ishizaka, K., Ishizaka, T., & Lee, E. H. (1970) *Immunochemistry 7*, 687–702.

Ishizaka, T., & Ishizaka, K. (1975) *Prog. Allergy 19*, 60–121.

Kanellopoulos, J. M., Liu, T. Y., Poy, G., & Metzger, H. (1980) *J. Biol. Chem. 255*, 9060–9066.

Kocher, H. P., & Spiegelberg, H. L. (1979) *J. Immunol. 122*, 1190–1195.

Kulczycki, A., Jr., & Metzger, H. (1974) *J. Exp. Med. 140*, 1676–1695.

Kulczycki, A., Jr., McNearney, T. A., & Parker, C. W. (1976) *J. Immunol. 117*, 661–665.

Laemmli, U. K. (1970) *Nature (London) 227*, 680–685.

Liu, F. T., Bohn, J. W., Ferry, E. L., Yamamoto, H., Molinaro, C. A., Sherman, L. A., Klinman, N. R., & Katz, D. H. (1980) *J. Immunol. 124*, 2728–2736.

Liu, F. T., Albrandt, K., Sutcliffe, J. G., & Katz, D. H. (1982) *Proc. Natl. Acad. Sci. U.S.A. 79*, 7852–7861.

Lowry, O. H., Rosebrough, N. J., Farr, A. L., & Randall, R. J. (1951) *J. Biol. Chem. 193*, 265–275.

Mercola, D., Morris, J., & Arquilla, E. (1972) *Biochemistry 11*, 3860–3873.

Metzger, H., Budman, D., & Lucky, P. (1976) *Immunochemistry 13*, 417–423.

Pecoud, A. R., Ruddy, S., & Conrad, D. A. (1981) *J. Immunol. 126*, 1624–1629.

Penefsky, H. S. (1977) *J. Biol. Chem. 252*, 2891–2899.

Perez-Montfort, R., & Metzger, H. (1982) *Mol. Immunol. 19*, 1113–1125.

Pick, U., & Karlish, S. J. D. (1980) *Biochim. Biophys. Acta 626*, 255–261.

Porter, R. R. (1959) *Biochem. J. 73*, 119–127.

Shaklai, N., Yguerabide, J., & Ranney, H. M. (1977) *Biochemistry 16*, 5585–5592.

Sippel, T. O. (1981) *J. Histochem. Cytochem. 29*, 1377–1381.

Siraganian, R. P. (1981) in *Cellular Functions in Immunity and Inflammation* (Oppenheim, J., Rosenstrich, D., & Potter, M., Eds.) pp 323–354, Elsevier/North-Holland, New York.

Snyder, B., & Freire, E. (1982) *Biophys. J. 39*, 137–146.

Sterk, A. R., & Ishizaka, T. (1982) *J. Immunol. 128*, 838–843.

Stryer, L. (1978) *Annu. Rev. Biochem. 47*, 819–846.

Takatsu, K., Ishizaka, T., & Ishizaka, K. (1975) *J. Immunol. 114*, 1838–1845.